Ultrasonic precursors to shear failure of rock joints in Gosford sandstone with rough contact surfaces

Gheibi, Amin
Department of Civil and Environmental Engineering, Colorado School of Mines, Golden, CO, USA
Hedayat, Ahmadreza
Department of Civil and Environmental Engineering, Colorado School of Mines, Golden, CO, USA

ABSTRACT: Ultrasonic wave measurements have been used as a remote and non-destructive method to monitor the changes in state of stress and slip initiation in rock joints. Although ultrasonic precursors in the form of maximum transmitted amplitude have been reported for gypsum and Indiana Limestone rock specimens, there is still more research needed for evaluation of causes and types of precursors on rock joints with rough contacting surfaces. We present results from novel ultrasonic compressional (P-) and shear (S-) wave propagation measurements in which sandstone rock joints with a non-homogenous contact roughness were sheared in a single direct shear setup under different sliding velocities. Our data show that depending on the sliding velocity and surface roughness, the transmitted amplitude may show a peak prior to the peak shear stress. However, some transducers follow a continuous decreasing trend with shear displacement which add complexities in detecting the seismic precursors. For the stick-slip cycles observed in the post peak region, the transmitted amplitude follows a cyclic trend consistent with shear stress fluctuations. Transmitted amplitude experienced a reduction during preparatory phase preceding to slip acceleration which led to identifying precursors in this mode of sliding.

1. INTRODUCTION

Frictional behavior of rock joints have been extensively investigated in previous numerical and experimental studies as a basis to understand the failure in rock slopes and movements of tectonic faults and subsequently earthquakes nucleation (Brace and Byerlee, 1966; Scholz, 2002; Jaeger et al., 2009; Khosravi et al., 2016, 2017). Slip initiation and propagation in rock discontinuities is dependent on multiple parameters related to material properties including material stiffness and surface roughness as well as the changes in loading environment e.g. sliding velocity and normal stress (Persson, 2013; Dorostkar et al., 2017; Leeman et al., 2018). In natural discontinuities with a non-homogenous and variable roughness, the normal stress and subsequently the shear stress is not distributed uniformly along the surface and therefore, slip may initiate from areas with low frictional strength and then propagate into areas with higher frictional strength (Hedayat et al., 2012; 2014a-d). Moreover, the variable roughness observed in natural rock joints affects the distribution of real contact area between the asperities at different locations, which is one of the main factors controlling the frictional strength as well as the sliding stability (Selvadurai and Glaser, 2017; Harbord et al., 2017). Several experimental methods such as acoustic emission, electrical resistivity, and seismic wave attenuation have been used to monitor sliding along faults and rock joints (Chen et al., 1993). However, the active seismic monitoring particularly compressional (P-) and shear (S-) wave propagation are considered as one of the most promising methods to monitor the local changes in physical properties of the rock joints (Hedayat et al., 2014a-c). Ultrasonic waves travel through the contact points between asperities and, thus, even the impact of small changes in the size and quality of contact as well as the volume of inter-particle voids could be represented in the ultrasonic wave attributes (Jia, 2000; Gheibi and Hedayat., 2018).

In recent studies, it has been observed that global shear failure in rock joints is the result of small localized failures at different locations of the joint (Jordan et al., 2011; Poli, 2017). These localized failures are taking place well prior to the main shear slippage/failure and generate precursory signals. Precursory signals carry valuable amount of insights about asperities failure and failure propagation along the rock joint. Thus, detecting the precursory signals could significantly help with

identifying frictional processes that also occur at larger scales in slope failures, landslides, and earthquakes.

Rock slopes may fail in different modes depending on the rock structure and changes in the loading conditions. The failure could be gradual with very slow movements or instantaneous slippage without much warning or indication. The slope failures could be triggered by different factors such as changes in pore water pressure or surcharge loads, however, the global failure is usually happening after the peak in shear stress is reached and detecting precursory signals prior to the peak shear stress would be necessary for prediction of macro scale slope failures. Hedayat et al. (2014a) identified seismic precursors to the peak shear stress in rock joints with homogenous and non-homogenous contact surfaces. They observed seismic precursors in transmitted both P- and S-waves prior to the peak shear stress. Depending on the shearing velocity, normal stress and material's roughness, rock joints may either fail in brittle mode showing peak in shear stress or in a soft mode without any peak. However, the appearance of seismic precursors with the changes in failure mode is still left unexplored.

In addition to rock slopes, the frictional behavior in tectonic faults is significantly influenced by the properties of rock joints and loading environment. Fast earthquakes are commonly modeled with unstable sliding as stick-slip motion, in which the slippages and sticking phases are considered as analog for the seismic and inter-seismic periods in natural tectonic faults (Brace and Byerlee, 1966). The prediction of earthquakes modeled by stick slip behavior is fascinating but a challenging topic (Soboley et al., 2001). Scuderi et al. (2016) identified seismic precursors in granular materials in a wide range of unstable sliding from slow slip to fast stick-slip cycles. Their study was focused on the granular gouge material confined between steel forcing blocks with homogenous roughness. However, in natural faults, the transmission of seismic waves is influenced by the surface roughness of rock joints and non-uniform distribution of contact area due to surface asperities. The changes in real contact area due to surface asperities exert additional challenges in detecting seismic precursors.

In this study, we aimed at identifying the ultrasonic precursors in rock joint samples during both stable and unstable sliding under different sliding velocities. Fractured rock joints from Gosford sandstone were sheared in a single direct shear device and simultaneously monitored by multiple ultrasonic P- and S- wave transducers. Samples were sheared up to the post peak and steady state condition.

2. LABORATORY EXPERIMENTS

The experimental setup used in this study is shown in figure 1. This configuration consists of a horizontal loading frame to provide the desired amount of normal stress, a vertical loading frame to apply the shear displacement, an assembly of transducer holder plates to place the transducers and a wave propagation system to record the transmitted waveforms through the material. In the following sections, the details of the experimental device and rock joints properties are described in details.

2.1. Single direct shear device

The single direct shear device consists of two independent devices: (a) a horizontal loading frame and (b) the main loading machine. In this setup, the rock joint sample is placed between transducer holder plates, which are confined between main steel plates with the load provided by the flat jack. Ultrasonic transducers are embedded in the transducer holder plate covered with a thin aluminum plate. The ultrasonic transducers are in touch with the outer side of the rock joints. After applying the normal stress, the horizontal frame with the sample assembly placed on the bottom platen of the main loading machine and the shear load is then applied on top of the sample by the steel load applier. A flat jack (ENERPAC RSM-500) was used to apply a constant normal stress during the experiment and was connected to a hydraulic pump with a closed loop servo-valve system. The system allowed for maintaining the desired confining pressure constant throughout the experiment. The amount of normal displacement (compaction and dilation) was measured with two horizontal linear Variable Differential Transformers (LVDTs) mounted on the sides of horizontal loading frame.

The shear experiments were conducted in displacement control mode with various range of sliding velocities. The loading machine used in this study has the maximum loading capacity of 700 kN. The amount of shear displacement or the shearing velocity was controlled by the feedback provided by three LVDTs mounted on the loading machine platen at 120 degrees. The corresponding shear stresses were measured by the pressure transducer inside the main loading frame with accuracy of 0.001 MPa. A special lubricant (Moly Anti-Seize) was used between the loading platen in the horizontal loading frame and the transducer holder plate to eliminate any friction between the two well-polished stainless steel surfaces. This has resulted in successful tests reported in previous studies (Aragon et al., 2018; Gheibi et al., 2018).

2.2. Ultrasonic Wave Acquisition System

A fast-ultrasonic wave imaging system was used to monitor the rock joint while it was subjected to shear displacement. Compressional, P- and shear, S- waves were transmitted across the joints using ultrasonic transducers housed inside the specially designed loading. Maximum 9 pairs of transducers could be embedded in the platens, but in order to increase the acquisition frequency to 2Hz, two arrays each including 5 transducers were placed on each side of the joint. Each source and

receiver platen contained 3 shear wave transducers and 2 compressional wave transduces. Figure 2 shows schematically the transducer layout that was used for seismic measurements.

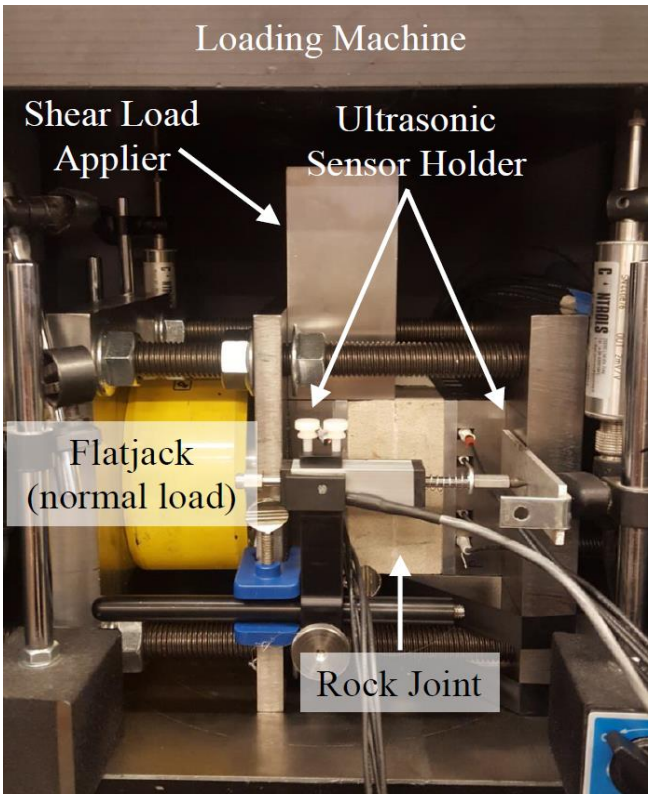

Fig. 1. Single direct shear setup used in this study. The horizontal loading frame with the confined rock joint is placed under the main loading machine.

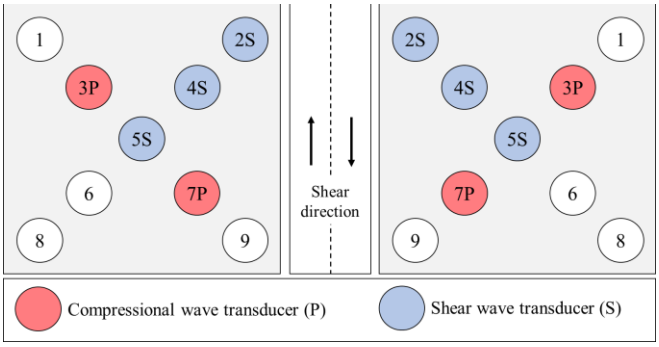

Fig. 2. The configuration of ultrasonic wave transducers (P- and S- waves).

The transducers were broadband with a central frequency of 1MHz (Panametrics V103RM for P-waves and V153RM for S-waves). A pulse generator (Panametrics 5077PR) was used for generating square-shape waveforms to provide input excitation for the source transducers. The input signal has the equal frequency as the transducer (1 MHz) and were sent with the repetition rate of 5 kHz and amplitude of 300 V. The data acquisition system recorded transmitted P- and S- waves every 0.5 second (sampling rate of 2 Hz).

The resolution of ultrasonic waves is dependent on the acoustical properties of material through which the waves are traveling as well as the coupling material and the contact stress between transducers surface and the rock joint. A thin layer of oven-baked honey at 90°C was used as the coupling layer between the transducers surface and the rock samples to improve the transmission of ultrasonic waves (Hedayat, 2013; Gheibi and Hedayat., 2018a,b). It is also important to keep the contact stress between the transducer and rock surface constant during the experiment. To achieve this, a spring washer and number of stainless-steel shims were embedded under each transducer in a way that final surface of every transducer was 2 mm higher than the final surface of aluminum cover plate. The washer acted as a spring and became flat under the preload stress and made the transducer to be at the same height as the aluminum cover plate.

2.3. Testing materials

In this study, the single direct shear experiments were conducted on Gosford sandstone. Gosford sandstone samples were sourced from Gosford Quarry, Somersby, New South Wales, Australia. Gosford sandstone forms a unit within the massive (*290 m* thick) Triassic Hawkesbury sandstone of the Sydney Basin (Ord et al. 1991) on the east coast of New South Wales, Australia. The unit occupies some *800 km*^{2} of the Sydney Basin and is typically composed of sub-angular to sub-rounded quartz grain, with argillaceous matrix, minor feldspar and clay (Ord et al., 1991, Aragon et al., 2018).

The samples were obtained from cores with no macro scale cracks or damage. The porosity of Gosford sandstone has been determined about 20% using X-ray CT scanning technique by Roshan et al. (2016, 2018). On the same batch of Gosford sandstone utilized in this study, X-ray diffraction method was conducted and the composition was determined as 86 % quartz, 7 % illite, 6 % kaolinite and 1% anatase (Masoumi et al., 2016). The reported maximum grain size of this sandstone is 0.6 mm., the Unconfined Compressive Strength (UCS) of Gosford sandstone with diameter of 50 mm and length/diameter ratio of 2 is reported about 52.3 MPa (Masoumi et al., 2016). For the same size, the average Young's Modulus (*E*) and Poisson's ratio of Gosford sandstone were reported as 12.1 GPa and 0.14, respectively (Masoumi, 2013; Aragon et al., 2018).

The rock joint samples were prepared according to Brazilian testing or split cylinder method (ASTM D-3967). In this method, two thin steel rods are first attached to the opposite sides of the cubic sample and then a compressional load is applied to fracture the sample into two pieces. The surface of the obtained samples has a non-uniform roughness while the surface asperities are well matched.

Surface roughness of rock joint samples were measured using laser profilometery technique. Figure 3 shows the surface roughness of one sample. Figure 4 is the histogram of the frequency distribution of surface asperities. Asperity heights have almost an approximately normal distribution and the maximum variation from the mean plane for the fractured surface is about 5 mm. The shear strength of a rock discontinuity is directly related to the surface roughness of the joint, and a higher shear strength is expected for samples with greater surface roughness.

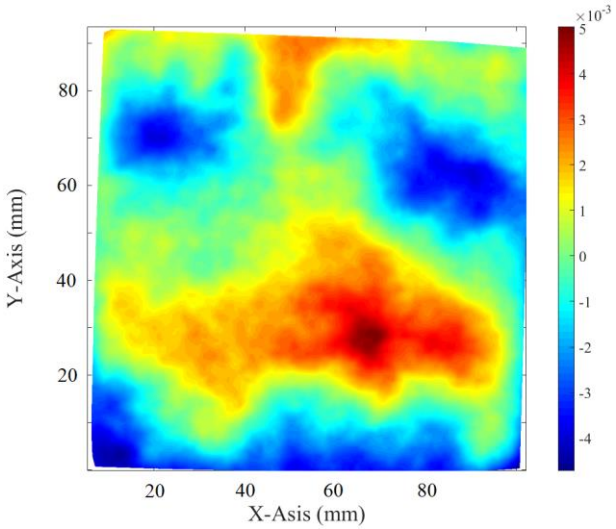

Fig. 3. Rock joints surface roughness in mm.

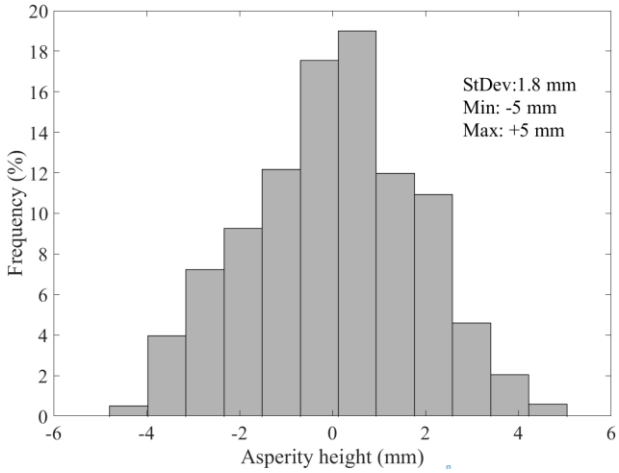

Fig. 4. Histogram of asperity heights.

3. RESULTS AND DISCUSSION

In this study, single direct shear experiments were conducted to explore the possibility of detecting seismic precursors to shear failure on fractured rock joints with variable surface roughness under different sliding modes and shearing velocities. Experiments were initiated with applying the desired level of normal stress which was then kept constant during the experiment. Due to the application of normal stress, the rock joints experienced compression and the contact area between the asperities increased. The normal stress was maintained constant for about 10 minutes to make sure that there is no additional compression and changes in contact area due to the new state of normal stress. After applying the compression load, the shear load was applied at constant shearing velocity on the moving side of the sample assembly, while the other side was fixed by the spacer as shown in figure 1. Up to the peak in shear stress, the samples were sheared at constant but different sliding velocities of 8 and 130 μm/s to investigate the role of sliding velocity on appearance of seismic precursors. In the post peak region, the sliding velocity was altered to cause unstable sliding and allows for evaluating the seismic precursors during stick-slip cycles. Ultrasonic measurements were conducted in all three stages of the experiments and the following sections were categorized according to the three different stages of 1) Compression; 2) Pre-peak stable sliding and 3) Post-peak stick-slip behavior.

3.1. Compression

During compression, the normal stress increased linearly from 0.2 MPa to 6 MPa and simultaneously transmitted compressional and shear waveforms were recorded. The rock joint thickness decreased with the increase in normal stress, however, the rate of changes was not constant and gradually decreased as the normal stress reached the target value, resulting a non-linear trend in thickness variation. Corresponding with the increase in normal stress and the decrease in joint thickness, the peak to peak amplitude of transmitted waves increased significantly, with the amplitude values at 6 MPa normal stress being about 30 times greater than the amplitude values obtained at 0.2 MPa normal stress. The trend of increase in P- and S- waves are not exactly similar, in fact, the nonlinear trend in variation of layer thickness was better observed in variation of peak to peak amplitude for P waves, indicating the sensitivity of compressional waves to the compressional deformation in rock joints. Similar sensitively was observed in the literature for thin layers of granular quartz sand (Gheibi and Hedayat, 2018).

The transmitted amplitude is a function of real contact area between asperities. The real contact area is dependent on multiple parameters including normal stress, material stiffness, porosity and stationery contact time between surface asperities (Kendall and Tabor, 1971; Nagata et al., 2008; Gheibi and Hedayat., 2018; Hedayat et al., 2018). The dependency of transmitted amplitude on the normal stress is clearly observed in the evolution of peak to peak amplitude with normal stress. The contact area also evolves logarithmically with time (Dieterich, 1978). As observed in figure 5, the transmitted amplitude slightly increases with time, while the normal stress is constant.

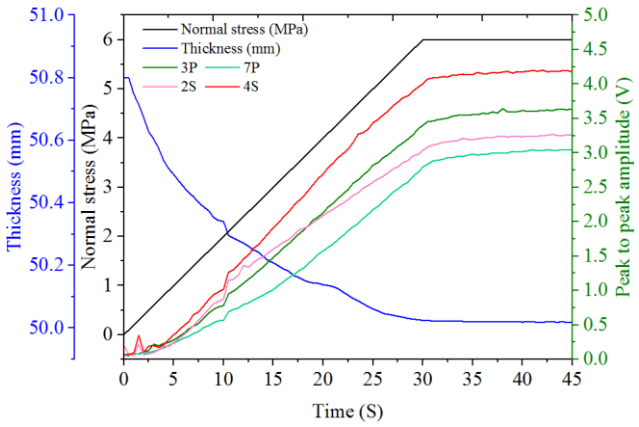

Fig. 5. Evolution of peak to peak amplitude for shear and compressional waves during the application of normal stresses.

3.2. Pre-peak stable sliding

After application of 6 MPa normal stress, the samples were sheared at two different constant shearing velocities of 8 and 130 µm/s. Figure 6 and 7 show the variation of shear stress and corresponding changes in transmitted amplitude with time. It was observed that the peak shear strength increases as the rock joint was sheared in a higher shearing velocity (130 µm/s), consistent with the behavior observed in the literature (Atapour and Moosavi, 2013). Also, with the higher shearing velocity, a sharper peak strength was observed in the shear stress data. However, the variation of transmitted amplitude may not necessarily follow a similar trend as the shear stress. The transmitted amplitude shows the local amount of changes in the real contact area between asperities, while the shear stress is the averaged contribution of shear stress from different contact areas along the surface.

The rock joints tested in this study had rough contacting surfaces, as shown in figure 3 and 4. The roughness significantly affects the variation of local contact area and subsequently the amplitude transmission. Depending on the location of transducer and the surface roughness pattern, ultrasonic peak to peak amplitude may experience increasing or decreasing trend. For the sliding velocity of 8 µm/s (figure 6a), the shear load is applied gradually and with a lower rate that the test with the sliding velocity of 130 µm/s, therefore the corresponding changes in peak to peak amplitude are more gradual. For the sliding velocity of 8 µm/s (figure 6a), transducer 3P shows a gradual increasing trend with a peak as the shear stress increases indicating the buildup of contact area due to shear deformation. However, the transducer 7P shows a continuous decrease. The observed peak in the transmitted amplitude of transducer 3P can be considered as the precursor to the peak shear strength of the interface. However, a different behavior was observed for both P-transducers in the experiment with 130 µm/s shearing velocity (figure 6b). For the sliding velocity of 130 µm/s presented in figure 6b and 7b, since the shear deformation is happening at a much higher rate, the transmitted amplitude first decreased suddenly. This initial decrease in transmitted amplitude is due to the breakage of contact points, which were developed during compression stage. After the initial drop (*t=3.5 to 5s*), the rate of changes in transmitted amplitude decreased and continued with the same rate up to the point where the next drop occurred.

The variation of amplitude for transducers that do not show a peak in transmitted amplitude can be categorized based on the changes in the slope of the amplitude curve. The change in the slope of transmitted amplitude shows the initiation of additional mechanisms leading to the loss of contact area which are hypothesized to be due to failure at localized contact points. The dashed lines fitted to the amplitude variations in figure 6 and 7 shows the constant slope in amplitude prior to the peak shear strength. The point that the amplitude deviates from the previous linear trend, marked by an orange arrow, was observed to happen close to the peak points in the transmitted amplitude for other transducers and could be considered as seismic precursors.

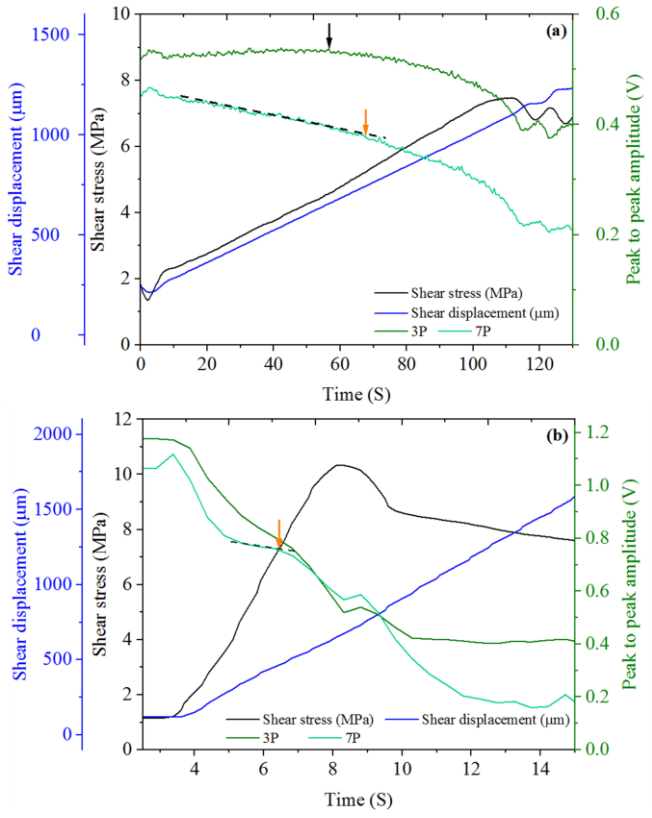

Fig. 6. Variation of shear stress, shear displacement and peak to peak P- wave amplitude prior to the peak shear strength and illustration of seismic precursors at two different sliding velocities a) 8 µm/s and b) 130 µm/s. Amplitude variations for both transducers are scaled on the same axis.

In addition to compressional waves, shear waves have been also used in other similar studies to identify seismic precursors. However, similar to the results obtained from P- waves, it is not always expected to observe similar

variations for transducers at different locations. The same methodology used to determine seismic precursors based on P- wave amplitude is also applied to S- wave data.

Figure 7 shows the variation of peak to peak amplitude for shear waveforms as well as the shear stress and shear displacement for two different sliding velocities. For shearing velocity of 8μm/s, transducer 5S showed a peak prior to the shear stress, which is identified as the precursor to the shear failure and for other transducers the point with slope change was determined as the precursor to the peak shear strength. Similar to the P-waves, peak to peak amplitude for shear waves experienced an initial drop due to the application of shear displacement. Followed to the initial drop, amplitude increased for two transducers of 2S and 5S in which the peak is determined as the seismic precursor. Transducer 4S showed a continuous decrease and did not produce any seismic precursors.

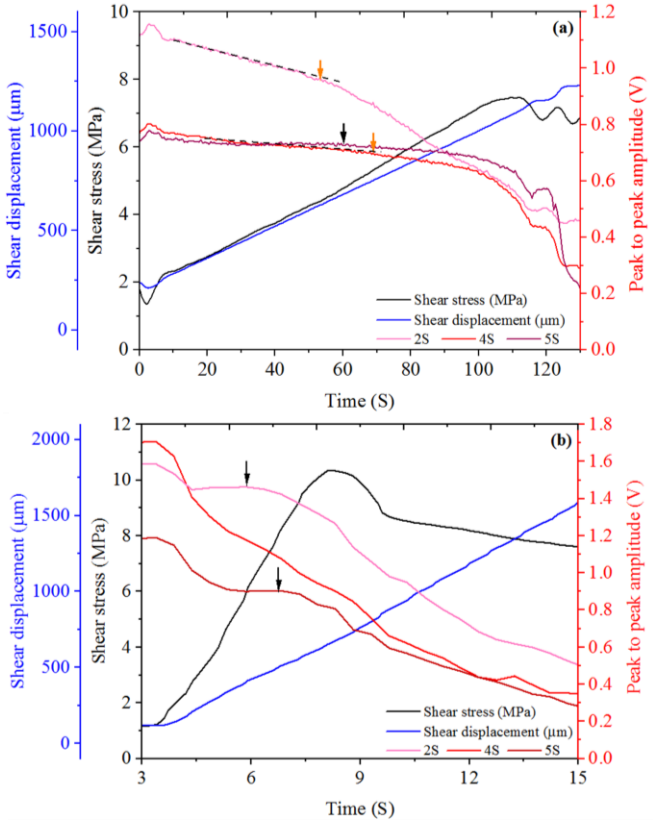

Fig. 7. Variation of shear stress, shear displacement and peak to peak S- wave amplitude prior to the peak shear strength and illustration of seismic precursors at two different sliding velocities a) 8 μm/s and b) 130 μm/s. Amplitude variations for all transducers are scaled on the same axis.

3.3. Post-peak stick-Slip behavior

The sliding mode and the transition between stable to unstable mode is one of the most complicated concepts in friction of geomaterials. The mode of sliding depends on several parameters and one single joint may experience both stable and unstable sliding under different loading conditions (Kato et al., 2012). Stick-slip behavior has been identified as the laboratory simulation of seismic and inter-seismic periods of natural tectonic faults. During stick-slip cycles, the interface sliding velocity is not constant and is fluctuating between lower and higher values than the defined load point velocity (Beeler et al., 1996).

Detecting precursors to peak shear stress during stick-slip cycles is challenging but a fascinating topic since it provide valuable information about predicting movements in tectonic faults. Scuderi et al. (2016) introduced the seismic precursors during slow and fast stick-slip cycles. The experiments were conducted on granular gouge material sandwiched between steel forcing blocks with uniform roughness. However, the non-uniform surface roughness for rock joint samples add additional complexities in detecting seismic precursors which has not been investigated in the literature. Figure 8 shows the variation of shear stress, shear displacement and corresponding changes in transmitted amplitude of shear and compressional waves at sliding velocity of 8 μm/s. The sliding velocity was equal to the sliding velocity prior to the peak shear strength, but the sample experienced unstable sliding. This is due to the changes in joint properties and changes in real contact area at the interface with cumulated shear deformation. Similar behavior has been observed in previous studies (Leeman et al., 2016; Leeman et al., 2018).

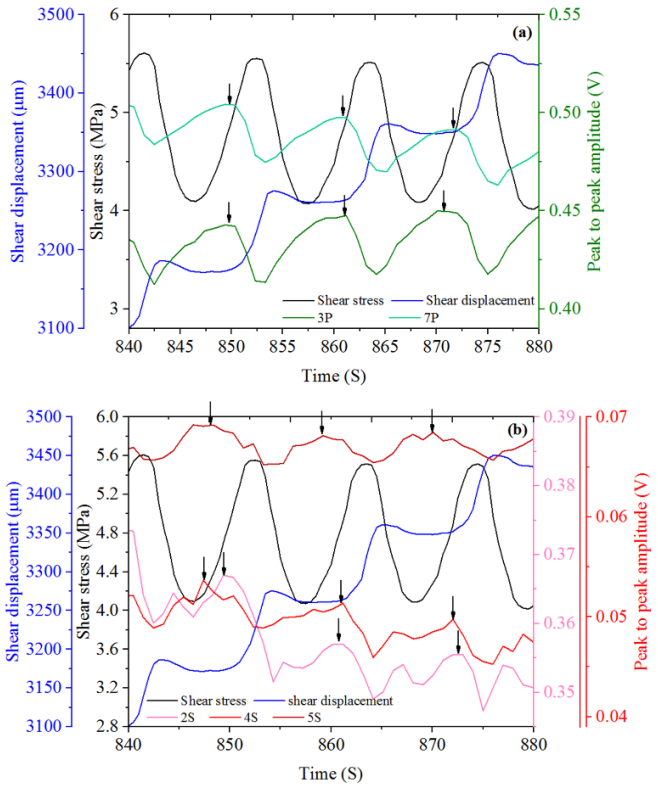

Fig. 8. Illustration of seismic precursors with respect to a) P-waves and b) S- waves peak to peak amplitude. Variation of shear stress, shear displacement and peak to peak P- and S-wave amplitude during three stick-slip cycles with average load point sliding velocity of 8 μm/s.

During stick-slip cycles, the transmitted amplitude showed cyclic trend with similar recurrence time as the shear stress; however, the peaks in transmitted amplitude were not coincident with the peaks in shear stress. Amplitude variations are due to the changes in real contact area between surface asperities. During the sticking phases (*845-850s, 855-860s, 866-871s*), the asperities were in touch and getting compressed, consequently the transmitted amplitude followed an increasing trend in this stage. However, as the slip initiated (*851, 861, 872*), the peak to peak amplitude started to decrease and continued to the point where maximum sliding velocity was reached. This observation was also reported in the work of Scuderi et al. (2016). Since the peak in transmitted amplitude corresponds to slip initiation and happened prior to the macroscopic shear failure, it can be considered as an appropriate measure to evaluate slip initiation or precursor to the shear failure. In figure 8, seismic precursors obtained from P- and S- waves are shown with black arrows for three different stick-slip cycles. P- wave transmitted amplitudes were observed to be more clear compared to the S- wave and more reliable values were obtained for precursors.

3.4. Precursors events

Seismic precursors can be elaborated as a function of time or displacement between precursors appearance and the peak in shear stress. To eliminate the impact of sliding velocity, the precursors were evaluated with respect to shear displacement rather than time.

Figure 9 shows the variations in appearance of precursors to the peak shear strength with the type of transducer, location of transducer and the sliding velocity. Precursors are varying between 150 to 270 µm for the sliding velocity of 130 µm/s and between 320 to 450 µm for the sliding velocity of 8 µm/s. The required amount of displacement for the peak shear stress, is 550 and 800 µm for the sliding velocities of 8 and 130 µm/s respectively. Therefore, the precursors appear within the range of 27 – 54% for 130 µm/s and 40 – 56 % for 8 µm/s. Precursors were observed to occur earlier for transducers located at top of the sample indicating the sequence of localized failure happening along the interface. The dashed lines in the figure 9 illustrate the sequence in precursor's appearance at different elevations.

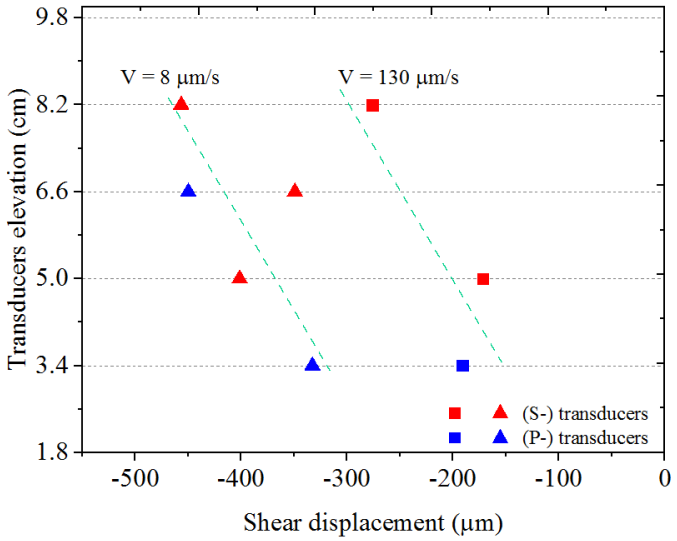

Fig. 9. Variation of seismic precursors to peak shear strength obtained from P- and S- waves for different sliding velocities along the interface.

The observed precursors during the stick-slip cycles had lesser variations compare to the precursors for the peak shear stress. This is attributed to the lower amount of shear deformation required to reach to the peak shear stress in stick-slip cycles. For the cycles shown in figure 8, the shear displacement happening in one cycle is about 90 µm and the recurrence time is about 11 seconds. Precursors appear about 30 µm and 2.5 seconds prior to the peak in shear stress. Since the sliding velocity during stick-slip cycles is not constant, the precursors are appearing about 30 % with respect to displacement and 22% with respect to time prior to the peak.

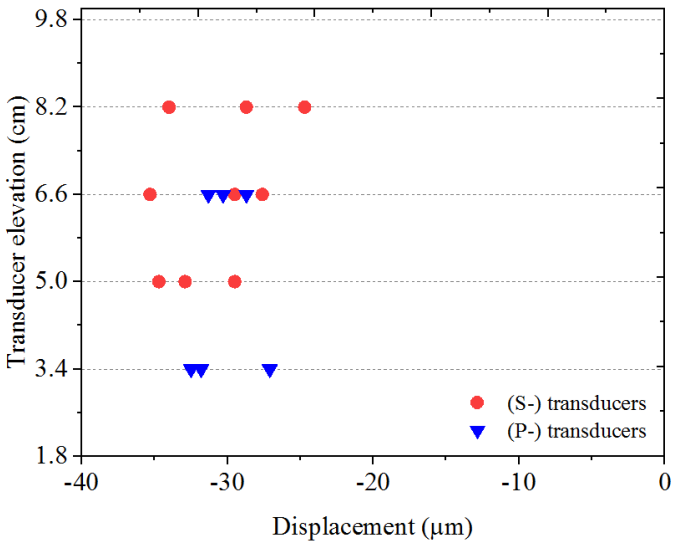

Fig. 10. Variation of seismic precursors during stick-slip cycles obtained from P- and S- waves for sliding velocity of 8 µm/s.

4. CONCLUSIONS

Direct shear experiments were carried out in this study to investigate the appearance of seismic precursors to the shear failure in rock joints with rough contacting surfaces. For this purpose, the Gosford sandstone rock joins were fractured according to the Brazilian method to have variable roughness at the joint. Samples were sheared in a single direct shear device equipped to ultrasonic wave propagation system to simultaneously monitor the joints surface as the samples were being subjected to shear displacement. The obtained results show different trends for variation of peak to peak amplitude for transducers at different locations, which is mainly due to the variable roughness along the surface. Prior to the peak shear stress, seismic precursors were determined as the peak in transmitted amplitude for those showing a peak, while for other transducers the point with the change in rate of amplitude variations was selected as the precursor. It was observed that the values obtained based on this method are close to the points with maximum transmitted amplitude. During stick-slip cycles, the cyclic variation in shear stress were also observed in the transmitted amplitude, indicating the potential in capturing seismic precursors during unstable sliding for rock joints with non-homogenous roughness.

5. AKNOWLEDGMENTS

The authors would like to acknowledge the support provided for this research by the Southern California Center through grant No. 17242.

6. REFERENCE

1. Aragón, L. E., A. Gheibi, H. Masoumi, and A. Hedayat, 2018. Geophysical Imaging of Frictional Contacts and Processes in Shaly Sandstone Rock Joints. *In 52nd US Rock Mechanics/Geomechanics Symposium. American Rock Mechanics Association*.
2. Atapour, H., and M. Moosavi. 2013. Some effects of shearing velocity on the shear stress-deformation behaviour of hard–soft artificial material interfaces. *Geotechnical and Geological Engineering* 31.5 (2013): 1603-1615.
3. Beeler, N. M., T. E. Tullis, M. L. Blanpied, and J. D. Weeks. 1996. Frictional behavior of large displacement experimental faults. *J. Geophysical Res. : Solid Earth*, *101*(B4), 8697-8715.
4. Brace, W. F., and J. D. Byerlee. 1966. Stick-slip as a mechanism for earthquakes. *Science*, *153*(3739), 990-992.
5. Chen, W.Y., C.W. Lovell, G.M. Haley, and L.J. Pyrak- Nolte. 1993. Variation of shear-wave amplitude during frictional sliding. *Int. Journal of Rock Mechanics and Mining Sciences and Geomechanics Abstracts*, 30: 779–784 .
6. Dieterich, J. H. 1978. Time-dependent friction and the mechanics of stick-slip. *Rock Friction and Earthquake Prediction* (pp. 790-806). Birkhäuser, Basel.
7. Dorostkar, O., R. A. Guyer, P. A. Johnson, C. Marone, and J. Carmeliet. 2017. On the micromechanics of slip events in sheared, fluid-saturated fault gouge. *Geophysical Research Letters*, *44*(12), 6101-6108.
8. Gheibi, A., and A. Hedayat. 2018a. Ultrasonic investigation of granular materials subjected to compression and crushing. *Ultrasonics*, 87, 112-125.
9. Gheibi, A., and A. Hedayat. 2018b. The Relation between Static Young's Modulus and Dynamic Bulk Modulus of Granular Materials and the Role of Stress History. *Proc. 5th Geotechnical and Earthquake Engineering and Soil Dynamics Conf, GEESDV. Austin. TX. Jun 10-13.*
10. Gheibi, A., S. Slouka, and A. Hedayat. 2018. Ultrasonic investigation of friction processes in granular gouge materials. *52nd US Rock Mechanics/Geomechanics Symposium*. American Rock Mechanics Association.
11. Harbord, C. W., S. B, Nielsen, N. De Paola, and R. E. Holdsworth. 2017. Earthquake nucleation on rough faults. *Geology*, 45(10), 931-934.
12. Hedayat, A., 2013. Mechanical and Geophysical Characterization of Damage in Rocks. Ph.D. *thesis, Purdue University, West Lafayette, IN.*
13. Hedayat, A., H. Haeri, J. Hinton, H. Masoumi, and G. Spagnoli. 2018. Geophysical signatures of shear induced damage and frictional processes on rock joint. *J. of Geophysical Res*. DOI: 10.1002/2017JB014773.
14. Hedayat, A., L. Pyrak-Nolte. and A. Bobet. 2014a. Precursors to shear failure of rock discontinuities. *Geophysical Research Letters*, 41, 5467-5475.
15. Hedayat, A., L. Pyrak-Nolte. and A. Bobet. 2014b. Detection and quantification of slip along non-uniform frictional discontinuities using digital image correlation. *Geotechnical Testing Journal*, 37 (5).
16. Hedayat, A., L. Pyrak-Nolte, and A. Bobet. 2014c. Multi-modal monitoring of slip along frictional discontinuities. *Rock Mechanics and Rock Engineering*, 47(5), 1575-1587, doi: 10.1007/s00603-014-0588-7.
17. Hedayat, A., L. Pyrak-Nolte. and A. Bobet. 2014d. Geophysical investigation of shear failure along cohesive-frictional rock discontinuities. *Proceedings of the 48th US Rock Mechanics Symposium, Minnesota, June 1-4.*
18. Hedayat, A., A. Bobet, and L. J. Pyrak-Nolte. 2012. Monitoring slip initiation and propagation along frictional interfaces with seismic wave transmission." *46th US Rock Mechanics/Geomechanics Symposium*. American Rock Mechanics Association,.
19. Kato, A., K. Obara, T. Igarashi, H. Tsuruoka, S. Nakagawa, and N. Hirata. 2012. Propagation of slow slip leading up to the 2011 Mw 9.0 Tohoku-Oki earthquake. *Science*, 1215141.
20. Kendall, K., and D. Tabor. 1971. An ultrasonic study of the area of contact between stationary and sliding surfaces. *In Proceedings of the Royal Society of London A: Mathematical, Physical and Engineering*

Sciences (Vol. 323, No. 1554, pp. 321-340). The Royal Society.
21. Khosravi, A., S. Mousavi, and A. D. Serej. 2016. Hydraulic behavior of infilled fractured rocks under unsaturated conditions. *Geotechnical and Structural Engineering Congress 2016* (pp. 1708-1718).
22. Khosravi, A., S. Mousavi, and M. A, Khosravi. 2017. Semi-Empirical Shear Strength Model for Infilled Rock Fractures with Infills in an Unsaturated State. *Geotechnical Frontiers* (pp. 529-538).
23. Jaeger, J. C., N. G. Cook, and R. Zimmerman. 2009. *Fundamentals of rock mechanics*. John Wiley and Sons.
24. Jia, X. 2000. Ultrasound propagation in disordered granular media. *MRS Online Proceedings Library Archive*, 627.
25. Jordan, T., Y.-T. Chen, P. Gasparini, R. Madariaga, I. Main, W. Marzocchi, G. Papadopoulos, G. Sobolev, K. Yamaoka, and J. Zschau. 2011. Operational earthquake forecasting: State of knowledge and guidelines for implementation, Ann. *Geophys*., 54(4), 315–391.
26. Leeman, J. R., C. Marone, and D. M. Saffer. 2018. Frictional mechanics of slow earthquakes. *Journal of Geophysical Research: Solid Earth*, 123, 7931–7949.
27. Leeman, J. R., D. M. Saffer, M. M. Scuderi, and C. Marone. 2016. Laboratory observations of slow earthquakes and the spectrum of tectonic fault slip modes. *Nature communications*, *7*, 11104.
28. Masoumi, H. 2013. Investigation into the mechanical behaviour of intact rock at different sizes, *in School of Civil and Environmental Engineering. UNSW Australia: Sydney, Australia*
29. Masoumi, H., S. Saydam, and P.C. Hagan. 2016. Unified size-effect law for intact rock. *International Journal of Geomechanics*, 16(2): 04015059.
30. Nagata, K., M. Nakatani, and S. Yoshida. 2008. Monitoring frictional strength with acoustic wave transmission. *Geophys. Res. Lett*. **35,** L06310.
31. Ord, A., I. Vardoulakis, and R. Kajewski. 1991. Shear band formation in gosford sandstone. *Int J Rock Mech Min Sci*, 28(5): 397-409.
32. Persson, Bo NJ. 2013. Sliding friction: physical principles and applications. *Springer Science and Business Media.*
33. Poli, Piero. 2017. Creep and slip: Seismic precursors to the Nuugaatsiaq landslide (Greenland). *Geophysical Research Letters* 44.17 (2017): 8832-8836.
34. Roshan, H., H. Masoumi, Y. Zhang, A.Z. Al-Yaseri, S. Iglauer, M. Lebedev, and M. Sarmadivaleh. 2018. Micro-structural effects on mechanical properties of Shaly-sandstone. *Journal of Geotechnical and Geoenvironmental Engineering.* 144(2): 06017019.
35. Roshan, H., M. Sari, H. Arandiyan, Y. Hu, P. Mostaghimi, M. Sarmadivaleh, H. Masoumi, M. Veveakis, S. Iglauer, and K. Regenauer-Lieb. 2016. Total porosity of tight rocks: A welcome to heat transfer technique. *Energy and Fuels*, 30(12): 10072-10079.
36. Scuderi, M. M., C. Marone, E. Tinti, G. Di Stefano, and C. Collettini. 2016. Precursory changes in seismic velocity for the spectrum of earthquake failure modes. *Nature geoscience*, 9(9), 695.
37. Scholz, C. H. 2002. The mechanics of earthquakes and faulting. *Cambridge university press.*
38. Selvadurai, P.A., and S.D Glaser. 2017, Asperity generation and its relationship to seismicity on a planar fault: A laboratory simulation: *Geophysical Journal International*, v. 208, p. 1009–1025.
39. Sobolev, K. Yamaoka, and J. Zschau 2011, Operational earthquake forecasting: State of knowledge and guidelines for implementation, *Ann*. *Geophys*., 54(4), 315–391.